

# Numerical simulation of flat-nose projectile penetrating concrete and soil target

DONG YONGXIANG, FENG SHUNSHAN

(State Key Laboratory of Explosion Science and Technology, Beijing Institute of Technology,  
Beijing 100081, China;)  
(Email: dongyongx@bit.edu.cn)

*Abstract:* The penetration into targets composed of concrete layer and semi-infinite foundation soil with flat-nose projectile is simulated with three-dimensional LS-Dyna finite element software. The deformation process and failure zone in the target are described. The penetration performance of projectile with flat nose is discussed. The penetration depth, the residual velocity and the deceleration amplitude of projectile increase with the initial velocity of projectile. And the penetrating cracks and the tensile crush zone indicate the damage of the target. The phenomena of concrete damage are in agreement with the experimental results.

Key-Words: numerical simulation; flat-nose projectiles; penetration performance; target

## 1 Introduction

Kinetic energy penetration is of importance in military application (terminal ballistics). A lot of work about Kinetic energy penetration into concrete targets has been done and pleasing achievements have been obtained [1-3]. Literatures [4-6] carried out on the penetration mechanism on concrete and literature [7-9] conducted numerical study of penetrating concrete targets.

The projectile nose shapes on the penetration has an important effect on the penetration characteristics. The penetration of the flat-nose projectile, as a blunt projectile into target is an interesting work to do. Although plenty of work about the penetration into concrete targets, but the work on the penetration into targets composed of concrete layer and semi-infinite foundation soil with flat-nose projectile is necessary. This paper studies the penetration characteristics of the flat-nose projectile into concrete layer and semi-infinite foundation soil with low velocity.

## 2 Problem description

Impact of projectile into targets involves in many factors, such as the initial velocity of projectile, mass of projectile, geometry of projectile (especially the nose of projectile), angle of attack and materials of the projectile, geometry and materials of target. Lots of experimental results on the penetration into concrete targets show that during the process of the penetration of the projectile into concrete targets, the surface of target adjacent to the position of impact will occur spalling because of the free surface effect of target and

shear and extrusion effect formed by projectile penetration into target.

The study problem by numerical simulation in this paper is the normal penetration of the flat-nose projectile into concrete layer and semi-infinite foundation soil.

The flat-nose projectile is 69 mm in diameter and 151 mm in length. The flat-nose projectile is made by 30CrMnSi and has a mass of 1.8 kg. The target is composed by concrete layer and semi-infinite foundation soil. The target is 500 mm in length and 500 mm in width. And the concrete is 100 mm in thickness. The thickness of foundation soil is taken 200 mm. The strength of concrete material is C20.

## 3 Numerical simulation

With the commercial software of LS-DYNA3D, the penetration of flat-nose projectile into targets composed of concrete layer and foundation soil is simulated.

### 3.1 Calculational Model

The calculation was carried out with the Lagrangian arithmetic. The geometric model is built with quarter part in numerical simulation because of symmetry of the load, the geometry of projectile and target, and boundary conditions. The calculational model includes the flat-nose projectile, concrete layer and foundation soil. The contact type of eroding\_surface\_to\_surface is adopted between the flat-nose projectile and concrete layer and the contact type of automatic\_surface\_to\_surface is used between concrete layer and foundation soil. The non-reflection

boundary condition is adopted in the lateral and bottom boundary of the target

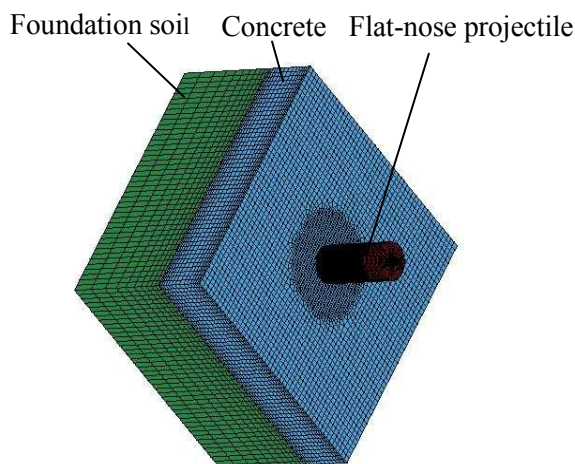


Fig.2 Finite element model of projectile and target

Fig.2 gives a diagram of discrete finite element model of flat-nose projectile and the combination target. The sizes of finite element model are shown in Fig.1. In a particular region, meshes are refined locally to obtain relatively reasonable results. The entire model includes 49,560 elements and 57,738 nodes.

### 3.2 Model Parameters

Because of the initial velocity and in order to check the strength properties of the flat-nose projectile, the kinematic hardening plastic constitutive model is used for the projectile and the elastic brittle model is adopted for concrete. The tensile stress failure criterion are used for the concrete. The SOIL\_AND\_FOAM model is used for the foundation soil [10]. Its yield function can be written as [11]

$$f = \frac{1}{2} S_{ij} S_{ij} - (a_0 + a_1 p + a_2 p^2)$$

Where  $a_0$ ,  $a_1$ ,  $a_2$  denote the material constant, respectively,  $p$  the pressure and  $S_{ij}$  the deviatoric stresses. The relationship between the pressure and the volumetric strain is given as

$$p = 8.626 \times 10^5 \times e^{18.9 \varepsilon_v^p}$$

The main material parameters are listed in Table 1-Table 3. Here  $\rho$  and  $E$  are density and elastic modulus,  $\mu$  the poisson's ratio,  $\sigma_b$ ,  $\sigma_c$  and  $\sigma_t$  the yield strength, the compressive strength and the tensile strength, respectively, BHN the hardening parameter,  $G$  and  $K$  the shear modulus and the bulk modulus.

Table 1 Material parameter of 30CrMnSi [12]

$\rho$ (g/cm <sup>3</sup> )	$E$ (MPa)	$\mu$	$\sigma_b$ (MPa)	$\sigma_c$ (MPa)	BHN
7.8	205.8	0.28	882	1078	420

Table 2 Material parameter of concrete [12, 13]

$\rho$ (g/cm <sup>3</sup> )	$E$ (GPa)	$\mu$	$G$ (GPa)	$\sigma_b$ (MPa)	$\sigma_t$ (MPa)
2.4	22.60	0.2	14.86	30	4

Table 3 Material parameter of soil [13]

$\rho$ (g/cm <sup>3</sup> )	$E$ (MPa)	$G$ (MPa)	$K$ (MPa)	$a_0$	$a_1$	$a_2$	$\mu$
1.8	47.38	16.01	394.8	2.4	13.6	0.1232	0.48

## 4 Simulation Results and Analysis

### 4.1 Analysis on action of projectile and target

Fig.3 shows the contours of pressure of the projectile and target of different time when the projectile normally penetrates the target with a velocity of 96 m/s. From Fig.3, it can be seen that penetration depth increases with the time and the zone of tensile damage on the upper surface of concrete expands with the increase of penetration depth. A small compressive zone is formed in the interface of concrete layer and foundation soil. When stress wave propagates into the soil, the amplitude of pressure is small.

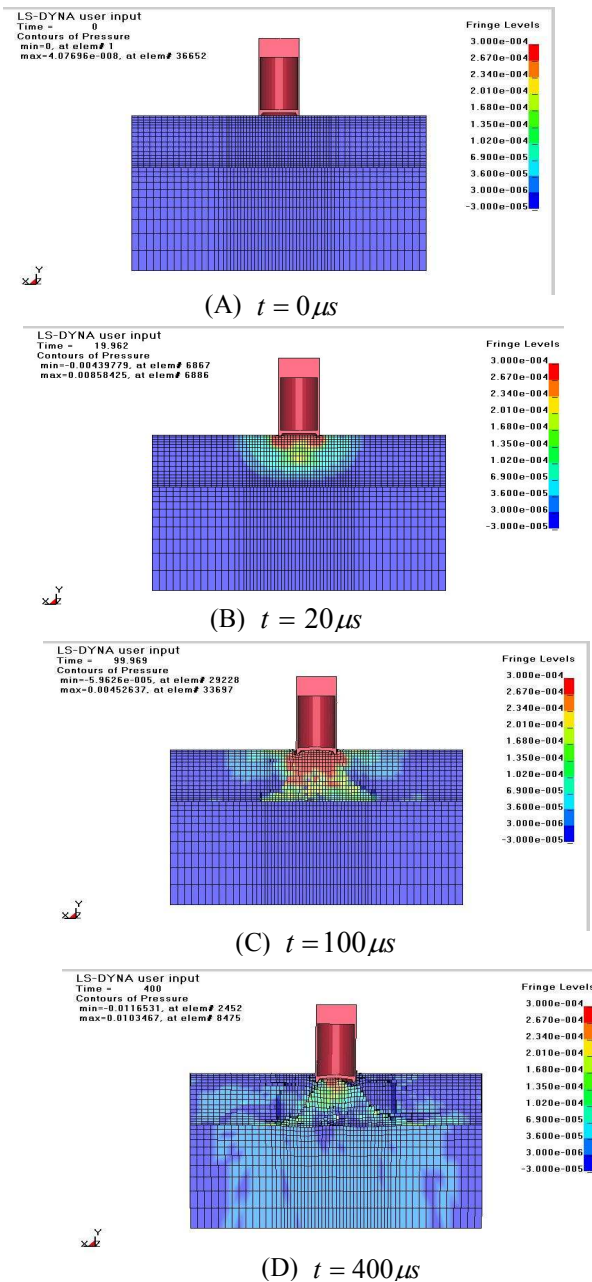


Fig.3 Contours of pressure as projectile penetrating into target

From the simulation results, it shows the penetration performance of the flat-nose projectile with the low impact velocity is weak. The penetration characteristics can use effectively in some special fields for the low penetration depth.

### 4.2 Failure analysis of targets

Fig.4 present the damage profiles of concrete layer by numerical simulation. It can be seen that after the impact of projectile, the crush zone is formed in the upper and bottom surface of the concrete. The crack zone is adjacent to the crush zone.

Fig.5 shows the damage profiles of concrete layer in the upper surface of the concrete by experiments under the same conditions with simulation work. Compared with Fig.5, it can be seen that the numeric results is in good agreement with the experimental result. Thus further study can be carried out to obtained more phenomena and conclusion by numeric simulation with less cost.

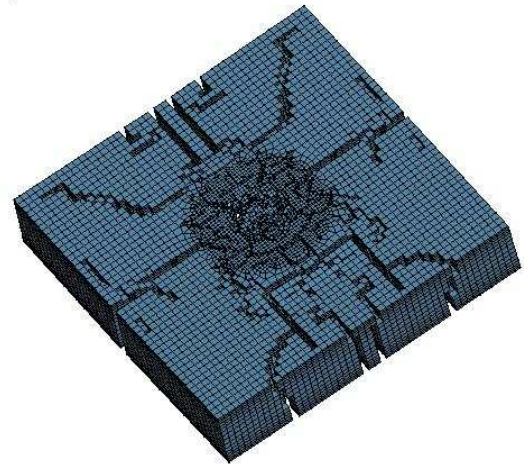


Fig.4 Damage profiles of the upper surface concrete layer by simulation

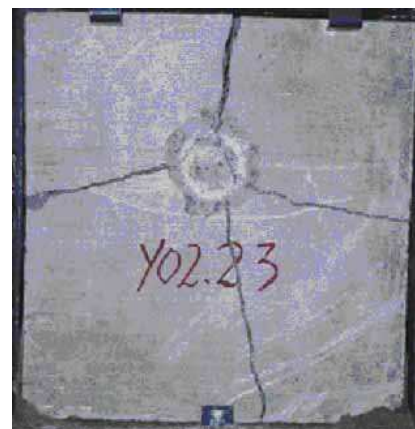


Fig.5 Experimental damage profiles of the upper surface in concrete layer

### 4.3 Penetration performance with different initial of projectile

By tracking the trajectory of the projectile, the time-displacement curve, the time-velocity curve and the time-deceleration curve at different impact velocity are obtained as shown in Fig.6, Fig.7 and Fig.8. From Fig.6, it can be seen that the penetration depth is less than 20mm when impact velocity change from 77m/s to 96m/s and the penetration depth increases with the impact velocity. Compared with Fig.4, it indicates that the penetration depth of projectile and the penetrating cracks and the tensile crush zone embody the damage of target.

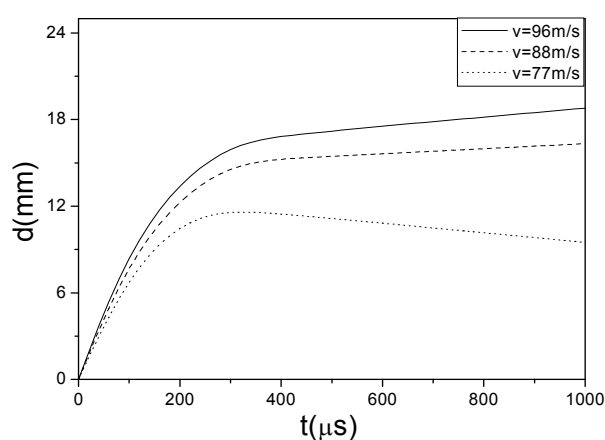


Fig.6 The curve of penetration depth with time at different impact velocity

Fig.7 shows the projectile velocity is very small after  $400\mu s$ . Compared with Fig.6, the increment of the penetration depth is small after  $400\mu s$  for different impact velocity. But when the impact velocity is 77m/s, the projectile velocity became negative after  $300\mu s$ . It indicated that after  $300\mu s$  the projectile began to rebound and the penetration depth decrease after it reaches the maximum.

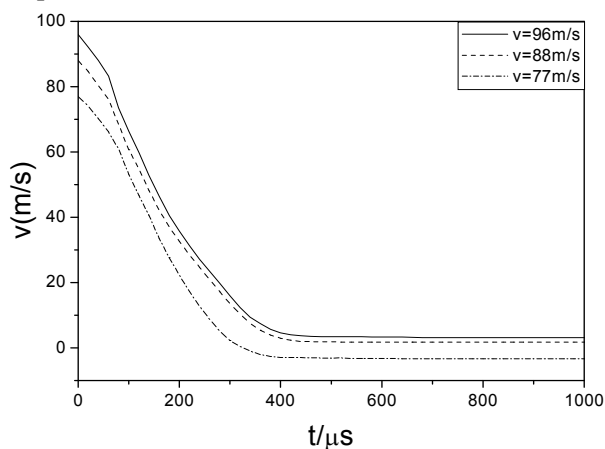


Fig.7 The curve of the projectile velocity with time at different impact velocity

Fig.8 shows the curve of the deceleration with time during penetration process. It indicates that the greater the velocity of the flat-nose projectile, the greater of the deceleration amplitude.

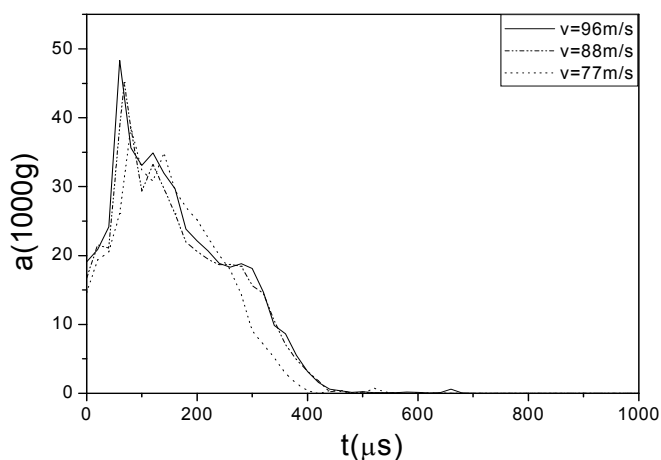


Fig.8 The curve of the deceleration with time at different impact velocity

## 5 Conclusions

By analysis of the projectile normally penetrating into target through numerical simulation, some conclusions are drawn as follows:

(1) Numeric result shows that the shape of the projectile's warhead has a certain effect on the penetration process. The flat-nose projectile has a strong impact on the target on the initial time in terms of the cutting ring. The impact velocity decreases with the entire contact of the projectile's warhead and target and the ultimate penetration capability is not prominent.

(2) In the numerical conditions of this paper, the deformation of the projectile is small which verifies its reliability of strength. When the target is composed of concrete layer and semi-infinite foundation soil, the impact mainly causes the damage of concrete in the upper layer. The damage zone of the concrete target includes the compressive crush zone in the center of the upper surface and the tensile crush zone in the center of the bottom surface in the concrete layer and the crack zone adjacent to the crush zone.

(3) The penetration depth increases with the impact velocity. The penetration depth of the projectile and the penetrating cracks and the tensile crush zone embody the damage of the target. The turning point in the beginning stage of the time-penetration depth curve indicates the cutting ring penetrates into target.

References:

[1] Luk V K, Forrestal M J. Penetration into Semi-infinite Rein-Forced-concrete Targets with

- Spherical and Ogival Nose Projectiles. *Int J Impact Engng*, 1987, 6(4) : pp. 291 - 301.
- [2] Forrestal M J . Penetration of Grout and Concrete Targets with Ogive-nose Steel Projectiles. *Int J Impact Engng*, 1996 ,18 (5) : pp. 465 - 476.
- [3] Q M Li, X. W Chen. Dimensionless formulae for penetration depth of concrete target impacted by a non-deformable projectile. *Int J Impact Engng*, 2003, 28(1): pp. 93-116.
- [4] Jan Arild Teland, Henrik Sjø. Penetration into concrete by truncated projectiles. *Int J Impact Engng*, 2004, 30(4): pp. 447-464.
- [5] Tomonori Ohno, Takashi Uchida, Noriyuki Matsumoto, Yoshihiko Takahashi. Local Damage of Reinforced Concrete Slabs by Impact of Deformable Projectiles. *Nuclear Engineering and Design*, 1992, 38(1): pp. 45-52
- [6] Eduardo Moreno Almansa, Manuel Fernández Cánovas. Behaviour of normal and steel fiber-reinforced concrete under impact of small projectiles. *Cement and Concrete Research*, 1999, 29(11): pp. 1807-1814.
- [7] C.Y. Tham. Reinforced concrete perforation and penetration simulation using AUTODYN-3D. *Finite Elements in Analysis and Design*, 2005, 41(14): pp. 1401-1410.
- [8] T.L. Teng, Y.A. Chu, F.A. Chang and H.S. Chin. Numerical analysis of oblique impact on reinforced concrete. *Cement and Concrete Research*, 2005, 27(4): pp. 481-492.
- [9] Yuh-Shiou Tai, Chia-Chih Tang. Numerical simulation: The dynamic behavior of reinforced concrete plates under normal impact. *Theoretical and Applied Fracture Mechanics*, 2006, 45(2): pp. 117-127.
- [10] Hallquist John O. LS-DYNA Theoretical Manual. Livermore Software Technology Corporation, 1998.
- [11] GU Wenbin; Ye Xushuang; Zhan Fami, etc. Dynamic Analysis on Spherical Charges Exploding in Semi-infinite Soil Medium. *Engineering Blasting*, 1999, 5(1) : pp. 5-10 ( in Chinese).
- [12] Liu Xiaohu; Liu Ji; Wang cheng; Dang Ruirong. Experimental Studies on the Projectile Penetrating Normally into a Plain Concrete, *Explosion and Shock Waves*, 1999 ,19(4) : pp. 323 - 328 ( in Chinese).
- [13] Holmquist T J, Johnson G R, Cook W H. A Computational Constitutive Model for Concrete Subjected to Large Strains, High Strain Rates and High Pressures. *14th International Symposium on Ballistics*, 1995, pp. 591-600.